ES Materials and Manufacturing
DOI: https://dx.doi.org/10.30919/mm1765

Phosphating of Carbon Steel in Solutions based on Technogenic Raw Materials

Sh. N. Kubekova,[1,*] V. I. Kapralova,[1] A. S. Raimbekova,[1,*] A. Dalbanbay,[1] Zh. Kuli,[1] A. B. Ibragimov[2] and A. Mukhanov[1]

Abstract

The properties of phosphate coatings formed on St3 carbon steel were investigated using calcium–manganese–phosphate solutions derived from Zhayrem ore beneficiation wastes and compared with conventional Mazhef salt solutions. Protective performance was evaluated using the drop method, gravimetric tests, and electrochemical techniques. Coatings obtained from the waste-derived solution at 85 °C for 60 minutes exhibited a protective capacity 1.5 times higher than those formed in Mazhef solutions. Electrochemical measurements confirmed this result, with corrosion current densities of 0.974 μA/ cm^2 for waste-derived coatings, compared to 1.623 μA/cm^2 for Mazhef coatings and 2.337 μA/cm^2 for uncoated steel. Gravimetric tests showed a lower mass loss over 8 days of immersion (0.0024 g vs. 0.0058 g). SEM and EDS analyses revealed that waste-derived coatings formed dense Ca–Fe–Mn–P layers with a thickness of ~11.1 μm, while Mazhef coatings were thinner (2.96–6.23 μm) and more porous. These findings demonstrate that manganese ore beneficiation wastes are an effective and sustainable source of phosphating agents for producing corrosion-resistant coatings on carbon steel.

Keywords: Carbon steel; Phosphate coating; Phosphating; Protective ability; Corrosion resistance.
Received: 16 July 2025; Revised: 15 September 2025; Accepted: 18 September 2025
Article type: Research article.

1. Introduction

Carbon steel is one of the most widely used structural materials in diverse industrial sectors, including mechanical engineering, the chemical industry, pipeline transport, and construction, owing to its high strength, ductility, ease of fabrication, and weldability.[1] Despite these advantages, its low intrinsic resistance to corrosion in aqueous and humid environments remains a critical limitation.[2] Corrosion of carbon steel not only leads to significant material loss and economic costs but also compromises the structural integrity and reliability of engineering systems.[2] Catastrophic failures of pipelines, steam boilers, storage tanks, and containers for toxic or reactive chemicals have been widely attributed to corrosion, highlighting the dual technical and environmental consequences of this phenomenon.[3] The release of corrosion products and transported substances into the environment further exacerbates ecological risks and raises concerns about industrial sustainability and safety.[4] For these reasons, the development of efficient, cost-effective, and environmentally responsible strategies for the corrosion protection of carbon steel continues to be a pressing global challenge.

Several strategies have been adopted to mitigate corrosion of steel and other ferrous alloys. These include alloy design through compositional modification to enhance inherent corrosion resistance, the application of protective organic or inorganic coatings to isolate the surface, control of the aggressiveness of the operating medium, and electrochemical protection methods such as cathodic protection.[5-7] Among these approaches, surface coatings have emerged as the most widely implemented solution, offering adaptability across a broad spectrum of industrial applications. Traditional organic coatings, such as paints and polymer-based films, are effective barriers but raise significant environmental and safety concerns due to their reliance on toxic solvents and their limited durability in aggressive environments.[8] In contrast, inorganic conversion coatings, particularly phosphate-based systems, are increasingly regarded as a more rational and sustainable alternative.

Phosphate coatings are formed through chemical treatment of metals with solutions containing phosphoric acid and its salts, resulting in the deposition of a crystalline phosphate layer that is chemically bonded to the underlying substrate[9-11] These coatings act as multifunctional layers and they improve corrosion resistance, enhance adhesion for subsequent paint or polymer layers, and reduce friction and wear. Their microcrystalline structure, composed of chemically bonded phosphate salts, provides a dense and

[1]*Kazakh National Research Technical University named after K.I. Satpayev – Satbayev University, Almaty, 050013, Kazakhstan*
[2]*Institute of General and Inorganic Chemistry, Tashkent, 100170, Uzbekistan*
[*]*Email:* s.kubekova@satbayev.university (Sh. N. Kubekova), a.raimbekova@satbayev.university (A. S. Raimbekova)

adherent barrier with microporous features that can be sealed or impregnated with organic or inorganic agents to further increase protective performance. The effectiveness of phosphate coatings, however, depends strongly on numerous parameters, including the composition and pH of the phosphating solution, the substrate alloy, treatment temperature and time, and post-treatment processes.[12,13] Although these coatings are primarily employed on ferrous alloys, recent developments have also extended their application to aluminum and magnesium alloys, expanding their technological relevance.[14,15]

Conventional phosphating solutions typically consist of orthophosphoric acid and salts of zinc or manganese, often supplemented with oxidizing agents such as nitrites, nitrates, chlorates, or permanganates to accelerate film formation and improve coverage uniformity.[15,16] Among them, the widely used "Mazhef" solution contains manganese and iron phosphates ($MnHPO_4$, $Fe(H_2PO1_4)_2$, $Mn(H_2PO_4)_2$) and is capable of producing high-quality phosphate layers on low-carbon steels.[17] However, preparation of such reagents requires production of specific salts through separate industrial processes that consume natural raw materials, which increases cost and resource intensity. In line with the principles of green chemistry and circular economy, the search for alternative sources of manganese- and calcium-containing phosphating agents, particularly those derived from industrial by-products and technogenic raw materials, has gained momentum in recent years.[18-20]

Kazakhstan possesses significant reserves of manganese ores, distributed across 19 deposits, with the Zhayrem deposit being one of the most prominent.[21,22] Industrial beneficiation of this ore is typically carried out by gravity separation, as flotation is ineffective due to the mineralogical characteristics of manganese ores. This process leaves behind considerable amounts of fine fractions enriched with manganese in tailings, which remain largely unutilized and present a growing geoecological concern. Valorization of these tailings as secondary raw materials for corrosion-protection technologies not only provides an avenue for waste recycling but also offers an economically attractive and environmentally sustainable pathway for producing phosphating solutions.[23] In a similar vein to recent studies on the valorization of natural resources for biomedical applications, such as the phytochemical profiling of Phlomis tuberosa L. for antioxidant and enzyme inhibitory potential, the search for sustainable, non-traditional sources of manganese- and calcium-containing phosphating agents reflects the same principles of green chemistry and circular economy.[24,25]

In this work, we explore the feasibility of using phosphate leachates derived from manganese ore beneficiation wastes of the Zhayrem deposit as a basis for preparing phosphating solutions. The formation of phosphate coatings on St3 carbon steel in these waste-derived solutions is systematically investigated and benchmarked against coatings produced using conventional Mazhef salt solutions. Comprehensive evaluation of the resulting coatings is conducted through accelerated corrosion tests, electrochemical methods, and detailed morphological and elemental analyses, providing insights into both the protective performance and the structural characteristics of the coatings. This study contributes to the development of eco-efficient corrosion protection strategies by integrating waste valorization with advanced surface engineering.

2. Materials and methods

2.1 Materials

Carbon steel specimens of grade St3 were employed, with the following chemical composition (wt%): 0.12 C, 0.20 Cr, 0.17 Mn, 0.025 P, 0.17 Si, 0.018 S, 0.25 Ni, 0.25 Cu, balance Fe. The specimens were cut into rectangular plates measuring 20 × 50 × 1 mm.

Before phosphating, all samples underwent surface preparation: mechanical polishing with fine-grain sandpaper, degreased with ethyl alcohol, rinsed with distilled water, and dried in a desiccator over calcined calcium chloride until constant mass was reached. The initial weight was determined with analytical balances (±0.1 mg), and surface area was recorded for normalization. All experiments were conducted in triplicate for reproducibility.

2.2 Methods

Protective performance evaluation

The protective performance of phosphate coatings was assessed by combining accelerated and long-term corrosion tests. Initially, the Akimov drop method was applied using a solution of $CuSO_4 \cdot 5H_2O$ (82 g/L), NaCl (33 g/L), and 0.1 N HCl (13 mL/L). A drop of this solution was placed on the coating surface, and the time required for a color change from gray to reddish-brown was recorded as an indicator of protective capacity.

Complementary corrosion resistance tests were carried out in accordance with standard procedures where coated specimens were exposed to corrosive aqueous media over extended periods, and the degree of coating degradation was monitored.[25] Together, these methods provided both rapid and long-term insights into the protective ability of the phosphate layers.

Electrochemical measurements

Electrochemical behavior was examined using a custom corrosion cell fabricated by 3D printing. The St3 working electrode was mounted to expose an active surface area of 1.54 cm^2 (14 mm diameter), with the remainder insulated. Tap water served as the electrolyte without added mineralization or neutralization, and tests were conducted at 20–25 °C under natural aeration.

The system employed an Ag/AgCl (3 M KCl) reference electrode and a graphite counter electrode. Prior to measurements, coated samples were immersed in tap water for 5 h to stabilize the corrosion potential (E_corr). Linear polarization scans were then conducted within ±150 mV of

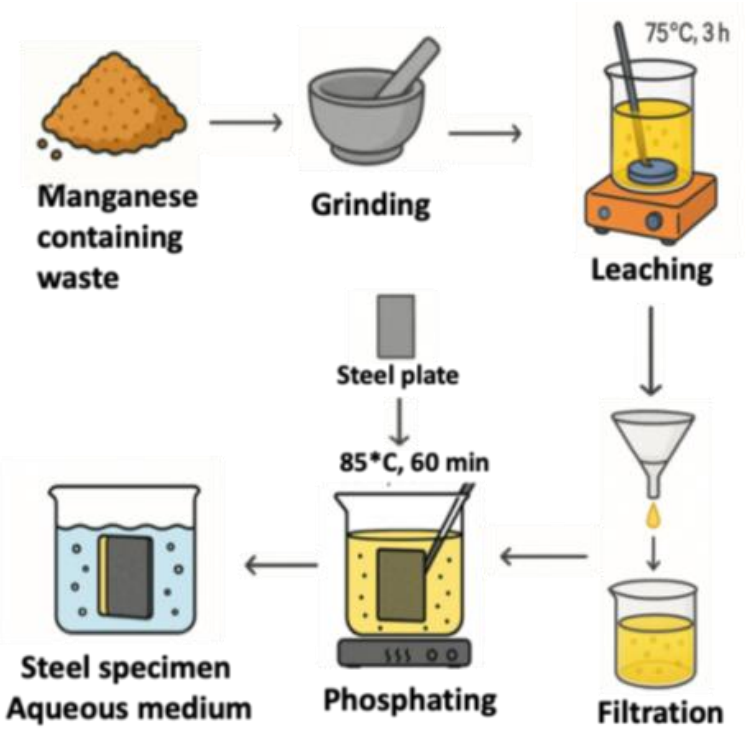


Fig. 1: Stages of carbon steel phosphating process in solution based on manganese ore beneficiation wastes.

Table 1: Chemical composition of manganese ore concentration wastes of Zhayrem deposit.

Spectrum	Content, wt% (stoichiometric oxygen, normalized)									
	Na_2O	MgO	Al_2O_3	SiO_2	SO_3	K_2O	CaO	TiO_2	MnO	FeO
Spectrum 1	0.66	1.71	3.03	20.02	0.71	0.71	61.71	0.36	9.14	1.95
Spectrum 2	1.22	1.77	4.07	31.56	0.78	0.59	52.53	0.43	5.21	1.84
Spectrum 3	1.01	1.21	3.40	21.43	1.78	1.01	49.02	0.91	16.02	4.21
Average	0.96	1.56	3.50	24.34	1.09	0.77	54.42	0.56	10.12	2.67
Std. Deviation	0.28	0.30	0.53	6.30	0.60	0.21	6.55	0.30	5.47	1.34
Max.	1.22	1.77	4.07	31.56	1.78	1.01	61.71	0.91	16.02	4.21
Min.	0.66	1.21	3.03	20.02	0.71	0.59	49.02	0.36	5.21	1.84

E_corr at 0.5 mV/s, starting in the cathodic direction.

Surface morphology and elemental analysis

Surface morphology of the coatings was characterized using a HITACHI TM3030 scanning electron microscope (SEM) equipped with a Bruker XFlash MIN SVE microanalysis system. Imaging was performed at accelerating voltages up to 15 kV with magnifications up to ×1500. Elemental mapping and distribution analysis were conducted via X-ray fluorescence microprobe scanning to determine the composition and uniformity of the phosphate layers.

3. Results and discussion

The phosphating behavior of carbon steel was investigated in solutions derived from phosphate leaching of manganese ore beneficiation wastes obtained from the Zhayrem deposit. Schematic representation of the experiments were shown in Fig. 1. X-ray diffraction (XRD) analysis of the raw waste material confirmed that the dominant crystalline phase is calcite ($CaCO_3$), constituting approximately 76.4 wt% of the sample. Other notable mineral phases include quartz (SiO_2, 16.4 wt%), albite ($NaAlSi_3O_8$, 4.8 wt%), and brownite ($Mn_2O_3{\cdot}3MnSiO_3$, 2.4 wt%), indicating that calcium-rich carbonates are the principal constituents, with silicates and manganese oxides occurring as minor but significant phases. A more detailed compositional characterization of the beneficiation wastes was carried out using electron-probe microanalysis (EPMA). The results are presented in Table 1, which shows the normalized stoichiometric oxygen-based chemical composition across three representative spectra. The data reveal that the wastes are enriched in calcium oxide (CaO,

49.02–61.71 wt%, average 54.42 wt%), confirming the dominance of calcite. High CaO concentrations, combined with measurable levels of silica (SiO_2, average 24.34 wt%), reflect the coexistence of carbonate and silicate phases. Minor components include MnO (5.21–16.02 wt%, average 10.12 wt%) and FeO (1.84–4.21 wt%, average 2.67 wt%), suggesting that although manganese and iron occur in lower concentrations than calcium, they remain critical for the subsequent formation of mixed phosphate coatings. Trace amounts of Al_2O_3 (3.03–4.07 wt%), MgO (1.21–1.77 wt%), Na_2O (0.66–1.22 wt%), K_2O (0.59–1.01 wt%), SO_3 (0.71–1.78 wt%), and TiO_2 (0.36–0.91 wt%) were also detected, with relatively narrow concentration ranges, which reflects their presence as accessory minerals such as feldspars and aluminosilicates.

The relatively high standard deviation observed for SiO_2 (±6.30 wt%) and MnO (±5.47 wt%) indicates heterogeneity in the distribution of quartz and manganese-bearing phases across different sampling points, whereas CaO, Na_2O, MgO, and FeO exhibit more consistent levels. This heterogeneity is typical of technogenic wastes, which are generated through beneficiation processes where mineral segregation is incomplete. From a functional perspective, the high CaO content is of particular interest, as during phosphate leaching it leads to the formation of $Ca(H_2PO_4)_2$, which does not occur in conventional Mazhef-type solutions. In fact, previous studies demonstrated that optimized leaching conditions yielded a phosphating solution containing $Ca(H_2PO_4)_2$ (98.2 g/L), $Mg(H_2PO_4)_2$ (2.3 g/L), $Mn(H_2PO_4)_2$ (10.0 g/L), $Al(H_2PO_4)_3$ (1.2 g/L), $Fe(H_2PO_4)_3$ (1.7 g/L), and free H_3PO_4 (7.8 g/L), with a total-to-free acidity ratio (Ct/Cf) of 13.5 and a solution pH of 1.10.[26] The critical distinction between this waste-derived phosphating solution and the conventional Mazhef reagent lies in the presence of calcium dihydrogen phosphate ($Ca(H_2PO_4)_2$), which establishes a unique stoichiometric ratio of $Mn(H_2PO_4)_2$:$Ca(H_2PO_4)_2$ ≈ 1:9.82. This compositional feature is expected to play a decisive role in the coating process by promoting the co-deposition of calcium-, manganese-, and iron-containing phosphates. As a result, the waste-based solution provides a more complex chemical environment than Mazhef, potentially enabling the formation of denser, less porous, and more corrosion-resistant conversion coatings on carbon steel.

The protective efficiency of phosphate coatings was assessed through the Akimov drop method, and the results are summarized in Table S1. Two different phosphating solutions were compared: a conventional Mazhef salt solution (pH 0.59) and a waste-derived phosphating solution from the Zhayrem deposit (pH 1.10). A clear correlation was observed between phosphating temperature, immersion time, and the protective capacity (PC) of the coatings. For both solutions, increasing the treatment time from 20 to 60 minutes resulted in a progressive improvement in protection. Similarly, raising the bath temperature from 65 to 85 °C significantly accelerated film growth and enhanced the corrosion resistance of the coatings. This behavior is consistent with the known temperature dependence of phosphate film nucleation and growth, where higher thermal energy facilitates ion transport, accelerates surface reactions, and promotes the formation of thicker and denser phosphate layers. Importantly, coatings formed in the Zhayrem waste-derived solution consistently outperformed those produced in the Mazhef solution across all treatment conditions. At 65 °C and 20 minutes, the protective capacity was 32 s in the waste-based solution compared to 25 s for Mazhef, while at 85 °C and 60 minutes, the waste-based coatings achieved a PC of 318 s versus 212 s for Mazhef, representing a 1.5-fold increase in protection. This improvement demonstrates the superior protective potential of the waste-derived solution, even under identical processing conditions. The higher protective capacity of the Zhayrem-based coatings can be attributed to their unique chemical composition. Unlike Mazhef, the waste-derived solution contains a substantial amount of calcium dihydrogen phosphate ($Ca(H_2PO_4)_2$) in addition to manganese and iron phosphates. The co-deposition of calcium along with manganese and iron phosphates likely contributes to the formation of mixed Ca–Mn–Fe phosphate films with lower porosity, greater thickness, and improved barrier properties against electrolyte penetration. Moreover, the higher solution pH (1.10 compared to 0.59 for Mazhef) may create more favorable conditions for uniform precipitation, reducing localized defects that serve as corrosion initiation sites. From a mechanistic perspective, at lower temperatures and shorter times, coatings are thin and discontinuous, providing limited resistance, as reflected in lower PC values. With increasing treatment severity, the coatings become progressively more compact and adherent, resulting in significantly higher PC values. The sharp increase observed for the Zhayrem solution at 85 °C for 40–60 minutes (230–318 s) suggests that the presence of calcium facilitates a more complete conversion reaction, leading to the formation of a dense phosphate layer with enhanced corrosion inhibition properties.

The accelerated corrosion test results were further validated using potentiodynamic polarization measurements (Fig. 2). The polarization curves provide detailed insights into the electrochemical behavior of carbon steel samples with and without phosphate coatings. The uncoated St3 reference sample displayed the highest anodic current density, corresponding to an active dissolution process without the presence of a protective barrier. This is reflected in the corrosion current density (I_corr) of 2.337 μA/cm^2, which translates to a corrosion rate of 0.0076 mm/year (Table 2). The corrosion potential (E_corr) for the bare steel was measured at –480.8 mV, indicating a relatively noble but unstable surface prone to localized attack.

By contrast, the sample coated in the Mazhef-based phosphate solution exhibited a significant reduction in corrosion current density to 1.623 μA/cm^2, lowering the

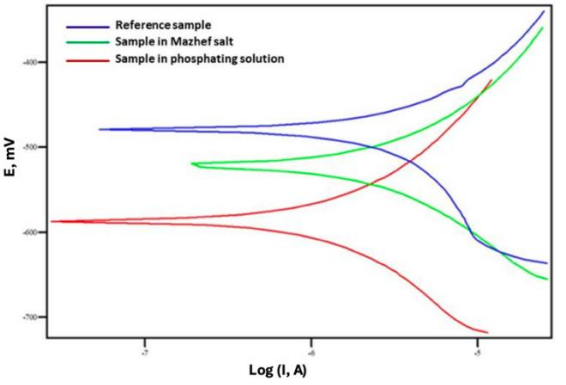


Fig. 2: Potentiodynamic polarization curves of uncoated St3 steel compared with phosphate-coated samples obtained from Mazhef solution and waste-derived phosphating solution.

Table 2: Electrochemical corrosion indicators of St3 with phosphate coatings formed in different solutions at 85 °C for 60 min.

Sample	Corrosion current density, μA/cm^2	Corrosion rate, mm/year	Corrosion potential, mV	Corrosion resistance as per EIS result, Ohm	Protective ability PC,%
Reference sample Ст3 without coating	2.337	0.0076	-480.8	1532	0.0
Phosphate coating formed in Mzhef salt	1.623	0.0053	-521.4	2037	30.6
Phosphate coating, formed in solution based on enrichment wastes	0.974	0.0032	-585.7	2348	58.3

corrosion rate to 0.0053 mm/year. This improvement corresponds to a protective ability of 30.6%, which is consistent with the formation of a Fe–Mn–P phosphate film that partially retards anodic dissolution. The polarization curve for this sample showed a slight negative shift in E_corr (–521.4 mV), indicating a more active but stabilized surface, likely due to increased uniformity in film coverage and partial passivation. Electrochemical impedance spectroscopy (EIS) confirmed this observation, with an increase in charge transfer resistance (R_ct) from 1532 Ω for bare steel to 2037 Ω for the Mazhef-coated sample, reflecting an enhanced barrier effect.

The most pronounced protective effect was observed inthe sample coated with the Zhayrem waste-derived solution, which achieved the lowest I_corr of 0.974 μA/cm^2 and a corresponding corrosion rate of 0.0032 mm/year. This represents a 58.3% improvement in protection, nearly double that of the Mazhef-based coating. The E_corr shifted further in the negative direction to –585.7 mV, suggesting stronger surface modification and the establishment of a stable passive layer that effectively suppresses anodic metal dissolution. The Tafel slope analysis revealed shallower anodic branches for this coating, which is characteristic of inhibited dissolution kinetics due to the presence of a dense and adherent phosphate layer. In line with this, the EIS data recorded the highest R_ct value of 2348 Ω, confirming the superior resistance of this coating to charge transfer and electrolyte penetration. The improved performance of the Zhayrem-derived coatings can be rationalized by their unique chemical composition. Unlike the Mazhef solution, which primarily deposits Fe–Mn phosphates, the waste-based solution incorporates significant amounts of $Ca(H_2PO_4)_2$ in addition to Mn and Fe phosphates. The co-deposition of calcium phosphates with iron and manganese phosphates likely enhances film compactness and reduces porosity, thereby limiting the diffusion pathways for aggressive ionic species (*e.g.*, Cl^-, H^+) into the steel/coating interface. This structural advantage translates into lower corrosion currents, higher polarization resistance, and overall superior protective efficiency.

Fig. 3 shows the Nyquist plots obtained by electrochemical impedance spectroscopy (EIS) for uncoated St3 steel and samples with phosphate coatings produced in Mazhef and Zhayrem waste-derived solutions. The uncoated sample displays the smallest semicircular arc, consistent with a low charge transfer resistance of 1532 Ω and poor corrosion resistance. The sample coated in the Mazhef solution exhibits a larger arc with a resistance of 2037 Ω, indicating moderateprotective ability, while the coating formed in the Zhayrem-derived solution provides the highest resistance of 2348 Ω, reflecting a more effective barrier to electrolyte penetration.

Equivalent circuit fitting revealed that the uncoated steel can be described by a simple R(RC) model, whereas coated

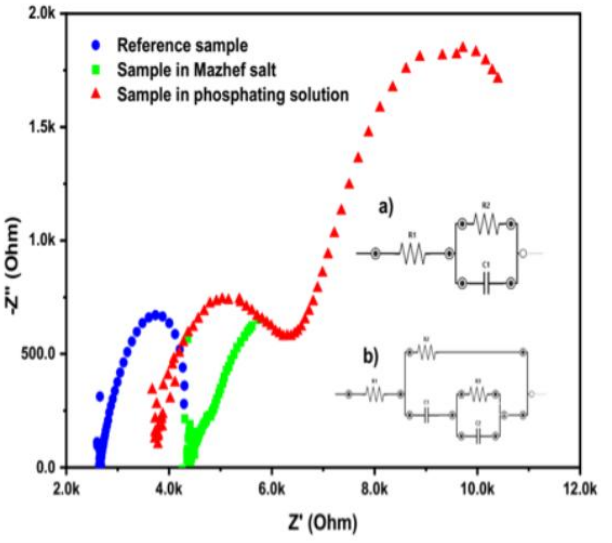


Fig. 3: Nyquist impedance diagrams of St3 samples with and without phosphate coatings in tap water, with equivalent circuit models for uncoated (a) and coated (b) specimens.

Table 3: Degradation of phosphate coatings in water, gravimetric tests.

Sample	Sample number	Test time, days			
		0	1	4	8
		Weight of steel samples, g			
PF, formed in solution based on enrichment wastes	1	7.8084	7.7877	7.7860	7.7856
	2	7.7249	7.7027	7.7018	7.7000
	3	7.6756	7.6548	7.6534	7.6526
Reference sample Ст3 without coating, control	4	7.1335	7.1298	7.1229	7.1170
	5	7.3218	7.3168	7.3101	7.3016
	6	7.1242	7.1190	7.1124	7.1044
PF, formed in the Mazhef salt	7	7.4848	7.4544	7.4495	7.4460
	8	7.2120	7.1887	7.1868	7.1838
	9	7.1570	7.1334	7.1322	7.1294

samples require a more complex R(RC)(RC) model, which accounts for the barrier properties of the phosphate film in addition to charge transfer at the metal interface. Calculation of protection efficiency confirmed that the Mazhef coating improved resistance by 33% compared to bare steel, whereas the Zhayrem-derived coating provided a 53% improvement. These results demonstrate that the calcium- and manganese-containing phosphates deposited from beneficiation wastes form denser and more protective layers than those obtained from conventional Mazhef solutions, in agreement with the polarization results.

The long-term protective performance of the phosphate coatings was further evaluated through gravimetric tests in accordance with standard requirements, which assess coating degradation under prolonged immersion in a corrosive medium. Steel specimens coated in phosphating solutions derived from Zhayrem enrichment wastes and Mazhef salt were exposed to tap water at 85 °C for up to 8 days, and their weight loss was monitored at intervals of 1, 4, and 8 days (Table 3, Fig. S1).

The results revealed that all coatings reduced mass loss compared to the uncoated reference samples, confirming their protective function. After the first 24 hours, the coating produced from Zhayrem waste exhibited a weight loss of 0.0212 g, which was approximately 1.2 times lower than that of the Mazhef-derived coating (0.0257 g). This difference widened with longer immersion: by day 8, the Zhayrem-based coating lost only 0.0024 g, whereas the Mazhef coating lost 0.0058 g, more than double the degradation observed in the waste-derived coating. The uncoated control specimens, as expected, showed the highest and continuous weight loss throughout the test, reflecting unimpeded corrosion in the

Table 4: Change in the elemental composition of phosphate coatings on the surface of steel samples after tests in water.

sample	Test time, days	Elemental composition, wt%				
		O	Fe	Ca	P	Mn
St3 without coating	8	37.54±0.26	58.16±0.55	0.00	0.00	0.30±0.22
PF based on enrichment waste	0	45.94±0.97	14.41±0.39	21.66±0.21	15.40±0.19	2.59±0.39
	8	38.14±0.74	30.89±0.37	15.49±0.20	13.85±0.20	1.62±0.37
PF based on Mazhef salt	0	22.57±0.42	55.20±0.43	0.00	9.67±0.29	12.56±0.44
	8	31.61±0.42	52.44±0.55	0.00	7.00±0.20	8.95±0.53

aqueous environment. These findings indicate that coatings formed in the Zhayrem waste-derived solution are more resistant to dissolution and better able to withstand prolonged water exposure compared to conventional Mazhef coatings. The improved stability can be attributed to the denser and more adherent microstructure of Ca–Mn–Fe phosphate phases formed from the waste solution, which reduces permeability and slows the ingress of corrosive species. In contrast, the Fe–Mn phosphate layers produced by the Mazhef solution are thinner and more porous, making them more susceptible to gradual degradation. Taken together, the gravimetric data reinforce the electrochemical measurements by confirming that phosphate coatings prepared from beneficiation wastes provide superior long-term protection in aqueous environments. The reduced weight loss over extended immersion times highlights the potential of technogenic raw materials as a sustainable and high-performance alternative for corrosion protection of carbon steel.

After 8 days of immersion in water, the steel samples were dried, qualitatively examined, and analyzed by scanning electron microscopy (SEM) coupled with energy-dispersive X-ray spectroscopy (EDS). Table 4 summarizes the elemental composition of the coatings before and after exposure. The phosphate coating formed in the Zhayrem waste-derived solution initially contained a high proportion of calcium (21.66 ± 0.21 wt%), phosphorus (15.40 ± 0.19 wt%), and manganese (2.59 ± 0.39 wt%), in addition to iron (14.41 ± 0.39 wt%) and oxygen (45.94 ± 0.97 wt%).

The high Ca content, exceeding the Fe content by a factor of ~1.5, reflects the incorporation of calcium dihydrogen phosphate species into the coating matrix, which distinguishes it from conventional Mazhef coatings that lack Ca-based phases. After 8 days of immersion, a clear decrease in Ca (to 15.49 wt%), P (to 13.85 wt%), and Mn (to 1.62 wt%) was observed, accompanied by an increase in Fe content (to 30.89 wt%). This suggests partial leaching of soluble dihydrogen phosphate species such as $Ca(H_2PO_4)_2$ and $Mn(H_2PO_4)_2$ into the aqueous medium, leaving behind a denser, Fe-rich phosphate network. In contrast, the Mazhef-derived coating showed lower initial Ca incorporation (absent altogether) and higher Fe content (55.20 wt%), with subsequent decreases in P and Mn after exposure, confirming its more porous and less stable nature compared to the Zhayrem-derived layer. These elemental changes explain the superior long-term corrosion resistance of the waste-based coatings, as the residual Ca–Mn–Fe phosphate framework resists dissolution more effectively than the predominantly Fe–Mn phosphate coating from Mazhef solutions.

The general morphology of the coating formed on the steel surface in the phosphating solution obtained during leaching of manganese-containing ore beneficiation wastes from the Zhayrem deposit indicates the formation of a fairly homogeneous dense layer, which explains its high protective properties. According to SEM microscopy, small vitreous agglomerates are observed on the surface in some places, probably from adsorbed calcium phosphates (Fig. 4A). In the process of holding this coating in water, its destruction occurs in the form of a violation of the continuity of the coating and the appearance of microcracks according to SEM microscopy (Fig. 4B). Although, most likely, the appearance of microcracks is associated with drying the sample in air to take micrographs. The incorporation of calcium phosphates plays a key role in enhancing compactness and reducing porosity, thereby improving both initial and long-term corrosion resistance compared to coatings formed in Mazhef-based solutions. The surface morphology of the phosphate coating formed on St3 in the Mazhef salt solution (Fig. 4C) reveals a layer composed of spherical crystals of varying sizes that assemble into agglomerates with a petal-like dendritic structure. Such morphologies are typically associated with preferential growth at the most corrosion-prone regions of the substrate, where localized electrochemical reactions driveuneven crystallization. After 8 days of immersion in water, noticeable degradation of the Mazhef-derived coatings was evident. SEM micrographs (Fig. 4D) revealed the formation of intergranular voids and microcavities, most likely due to the leaching of soluble $Fe(H_2PO_4)_3$ and $Mn(H_2PO_4)_3$ phases into the aqueous medium.

Elemental mapping results (Fig. S2) corroborated these findings, revealing that the Zhayrem-derived coating was uniformly enriched with Ca, P, and Mn distributed alongside Fe and O. This homogeneous distribution of multiple protective species creates a dense microstructure with reduced porosity, improving the barrier effect against corrosive agents.

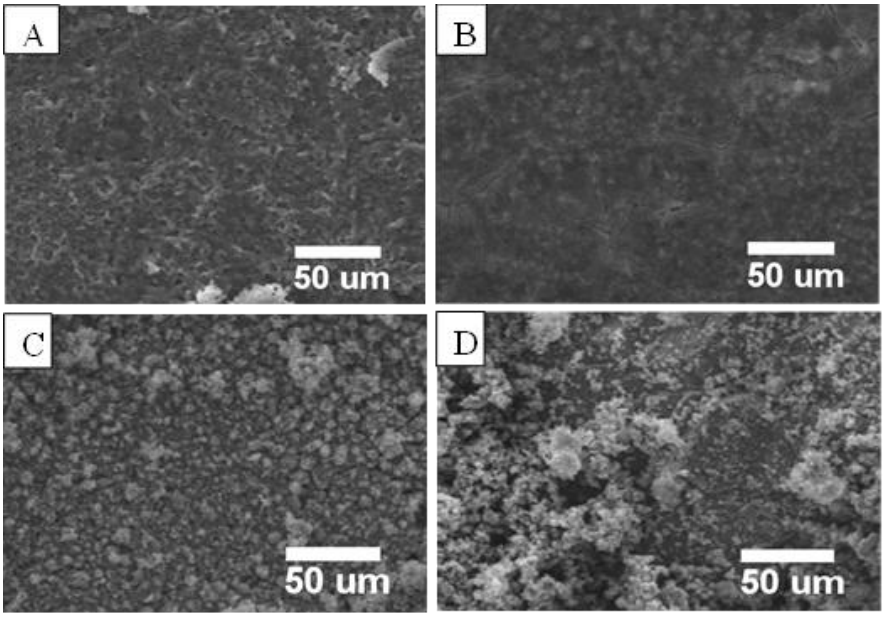


Fig. 4: Microstructure of phosphate coating formed on St3 in Mzhef salt solution before tests in water (A) and after tests (B) and microstructure of phosphate coating formed on Ct3 in phosphating solution based on enrichment wastes before tests (C) and after tests in water (D).

The decline in Ca, Mn, and P after immersion is consistent with the migration of more soluble phosphate phases into solution, but the persistence of significant amounts of these elements after 8 days highlights the durability of the waste-derived coating. Cross-sectional SEM images (Fig. S3) provided further insights into coating stability. Initially, the Zhayrem-derived coating exhibited an average thickness of 15.74 ± 18.57 µm (Fig. S3(A)), forming a compact layer strongly adhered to the steel substrate by following the standard test method.[27,28] After 8 days of immersion, the coating thickness decreased to 11.11 ± 14.14 µm (Fig. S3(B), S3(C)). This reduction can be attributed to the partial dissolution of adsorbed and weakly bound $Ca(H_2PO_4)_2$ and $Mn(H_2PO_4)_2$ phases, consistent with the EDS results. Nevertheless, even after degradation, the coating retained considerable thickness and structural integrity, demonstrating its ability to provide long-term protection.[29] Taken together, the results from Table 4, Fig. S2 and S3 demonstrate that phosphate coatings derived from manganese beneficiation wastes form a dense Ca–Mn–Fe–P protective layer, which undergoes controlled compositional adjustment during immersion but maintains a stable barrier against corrosion. Visual inspection of the Mazhef-based coatings suggested a relatively uniform surface; however, detailed SEM and elemental mapping analyses demonstrated that the deposits are predominantly composed of Fe–Mn–P phases (Fig. S4, Table 5). This interpretation is supported by elemental mapping, which showed a ~1.4-fold reduction in both phosphorus and manganese content (Table 4), confirming preferential dissolution of these phosphate species. Cross-sectional SEM analysis provided further insights into coating thickness and structural integrity (Fig. S5). The initial Fe–Mn phosphate coating produced in the Mazhef solution exhibited a thickness of only 6.36–6.61 µm (Fig. S5(A)), which is substantially thinner than the Ca–Fe–Mn phosphate coatings obtained in Zhayrem-derived solutions. After 8 days of immersion, the thickness of the Mazhef-based coatings decreased further to 2.96–6.23 µm (Fig. S5(B)), accompanied by an increase in porosity. The absence of $Ca(H_2PO_4)_2$ in the Mazhef solution explains the relatively weak structure of these coatings. Their formation is primarily governed by the anodic generation of Fe^{2+} ions, which react with $H_2PO_4^-$ to form $Fe(H_2PO_4)_2$, followed by hydrolysis to $FeHPO_4$ at anodic sites, while $MnHPO_4$ crystallization occurs at cathodic sites. These crystallites merge to form an Fe–Mn–P film; however, due to the lack of calcium phosphate incorporation, the resulting coating is thinner, more porous, and less protective than the Ca–Fe–Mn–P films produced in Zhayrem waste-derived solutions. Overall, the obtained results demonstrate that phosphate coatings formed in Mazhef solutions are structurally inferior to those produced from enrichment waste solutions. The reduced thickness, higher porosity, and compositional instability of Mazhef coatings explain their lower corrosion resistance compared to the dense, calcium-enriched coatings obtained from Zhayrem-derived solutions. These findings highlight the dual advantages of waste-based phosphating solutions: enhanced corrosion protection and sustainable valorization of technogenic raw materials, thereby improving both the technical and geoecological performance of phosphating processes.

4. Conclusion

This study demonstrates the feasibility of using phosphate leaching solutions derived from manganese ore beneficiation wastes of the Zhayrem deposit to produce high-performance anticorrosion coatings on carbon steel. Comparative analysis

with conventional Mazhef-based solutions highlights the superior protective properties of the waste-derived coatings. Accelerated testing showed that the protective capacity of coatings formed on St3 in the Zhayrem waste solution at 85 °C for 60 minutes was approximately 1.5 times higher than that of coatings produced in Mazhef solutions. Electrochemical characterization confirmed these findings: the corrosion current density decreased from 2.337 μA/cm² for bare steel to 1.623 μA/cm² for Mazhef coatings, and further to 0.974 μA/cm² for coatings formed in the waste-derived solution. Impedance modeling revealed corresponding increases in charge transfer resistance, from 1532 Ω for uncoated steel to 2037 Ω for Mazhef coatings and 2348 Ω for waste-based coatings, underscoring their enhanced barrier performance. Gravimetric tests over 8 days of immersion in water further validated the long-term stability of the Zhayrem-derived coatings. The total mass loss was limited to 0.0024 g, less than half of the 0.0058 g observed for Mazhef coatings under identical conditions, indicating greater resistance to aqueous degradation. Morphological and compositional analyses revealed that the waste-derived coatings consist of a dense, crystalline Ca–Fe–Mn–P layer with an average thickness of 11.11 ± 14.14 μm, whereas Mazhef coatings formed thinner and more porous Fe–Mn–P films of only 2.96–6.23 μm. The incorporation of calcium phosphate phases into the waste-based coatings reduces porosity, improves compactness, and significantly enhances corrosion resistance. Taken together, these results establish that manganese ore beneficiation wastes represent a valuable secondary raw material for the production of phosphate coatings. Their use not only improves the technical and economic efficiency of the phosphating process but also provides an environmentally sustainable route for valorizing industrial wastes while reducing geoecological risks.

Acknowledgments

This work was carried out within the framework of the research project AP23489432 entitled “New conversion anti-corrosion coatings based on waste from the enrichment of manganese ores in Kazakhstan” for 2024–2026, funded by the Science Committee of the Ministry of Science and Higher Education of the Republic of Kazakhstan.

Conflict of Interest

The authors declare that there is no conflict of interest.

Supporting Information

Applicable.

CRediT Statement

Sh. N. Kubekova and **A. S. Raimbekova:** Conceptualization, Supervision, Project administration, Funding Acquisition. **V. I. Kapralova** and **A. Dalbanbay:** Methodology, Software. **Zh. Kuli:** Formal analysis. **Zh. Kuli**, **A. B. Ibragimov** and **A. Mukhanov:** Investigation, Resources, Data curation. **Sh. N. Kubekova** and **A. S. Raimbekova** Writing-Original draft preparation, Writing-Review and Editing. All authors have read and agreed to the published version of the manuscript.

References

[1] O. Falodun, S. Oke, M. Bodunrin, A comprehensive review of residual stresses in carbon steel welding: formation mechanisms, mitigation strategies and advanced post-weld heat treatment techniques, *The International Journal of Advanced Manufacturing Technology*, 2025, **136**, 4107-4140, doi: 10.1007/s00170-025-15088-8.

[2] D. Dwivedi, K. Lepková, T. Becker, Carbon steel corrosion: a review of key surface properties and characterization methods, *RSC Advances*, 2017, **7**, 4580-4610, doi: 10.1039/C6RA25094G.

[3] M. Wasim, M. B. Djukic, External corrosion of oil and gas pipelines: a review of failure mechanisms and predictive preventions, *Journal of Natural Gas Science and Engineering*, 2022, **100**, 104467, doi: 10.1016/j.jngse.2022.104467.

[4] T. Prošek, P. Keil, K. Popova, Corrosion protection and sustainability: why are the two concepts inherently intertwined, *Corrosion and Materials Degradation*, 2025, **6**, 38, doi: 10.3390/cmd6030038.

[5] D. G. Răuță, E. Matei, S.-M. Avramescu, Recent development of corrosion inhibitors: types, mechanisms, electrochemical behavior, efficiency, and environmental impact, *Technologies*, 2025, **13**, 103, doi: 10.3390/technologies13030103.

[6] H. S. Aljibori, A. Alamiery, and A. A. H. Kadhum, Advances in corrosion protection coatings: A comprehensive review, *International Journal of Corrosion and Scale Inhibition*, 2023, **12**(4), 1476-1520, doi: 10.17675/2305-6894-2023-12-4-6.

[7] Z. Guo, Z. Xiao, H. Chen, X. Zhou, P. Wang, J. Luo, Y. Gao, H. Shang, Review of cathodic protection technology for steel rebars in concrete structures in marine environments, *Applied Sciences*, 2024, **14**, 9062, doi: 10.3390/app14199062.

[8] R. Shults, Geodetic substantiation of the Saryarka copper ore region, News of the National Academy of Sciences of the Republic of Kazakhstan, *Series of Geology and Technical Sciences*, 2020, **6**(444), doi: 10.32014/2020.2518-170X.147.

[9] P. Saik, O. Cherniaiev, O. Anisimov, K. Rysbekov, Substantiation of the direction for mining operations that develop under conditions of shear processes caused by hydrostatic pressure, *Sustainability*, 2023, **15**, 15690, doi: 10.3390/su152215690.

[10] S. Silva-Fernández, B. Díaz, R. Figueroa, X. R. Nóvoa, C. Pérez, A comprehensive structural and electrochemical study on the performance of Mn-phosphate layers, *Surface and Coatings Technology*, 2024, **476**, 130260, doi: 10.1016/j.surfcoat.2023.130260.

[11] D. Ernens, G. Langedijk, P. Smit, M. B. de Rooij, H. R. Pasaribu, D. J. Schipper, Characterization of the adsorption mechanism of manganese phosphate conversion coating derived tribofilms, *Tribology Letters*, 2018, **66**, 131, doi: 10.1007/s11249-018-1082-2.

[12] D. Saran, A. Kumar, S. Bathula, D. Klaumünzer, K. K. Sahu, Review on the phosphate-based conversion coatings of

magnesium and its alloys, *International Journal of Minerals, Metallurgy and Materials*, 2022, **29**, 1435-1452, doi: 10.1007/s12613-022-2419-2.
[13] A. Kumar, K. Verma, D. Rajput, V. Dhayal, A. Biswas, Recent Advances in Phosphatization of Metals for Corrosion Protection, *NanoWorld J*, 2003, **9**(S5), S373-S379, doi: 10.17756/nwj.2023-s5-066.
[14] M. A. Hafeez, A. Farooq, A. Zang, A. Saleem, K. M. Deen, Phosphate chemical conversion coatings for magnesium alloys: a review, *Journal of Coatings Technology and Research*, 2020, **17**, 827-849, doi: 10.1007/s11998-020-00335-2.
[15] D. Saran, A. D. Pathak, D. Klaumünzer, S. Bathula, K. K. Sahu, Novel perspectives on the mechanism of phosphate conversion coating on magnesium alloys, *Results in Surfaces and Interfaces*, 2024, **16**, 100243, doi: 10.1016/j.rsurfi.2024.100243.
[16] B. Herbáth, K. Kovács, M. Jakab, É. Makó, Crystal structure and properties of zinc phosphate layers on aluminum and steel alloy surfaces, *Crystals*, 2023, **13**(3), 369, doi: 10.3390/cryst13030369.
[17] E. Rumyantsev, V. Rumyantseva, V. Konovalova, White phosphate coatings obtained on steel from modified cold phosphating solutions, *Coatings*, 2022, **12**(1), 70, doi: 10.3390/coatings12010070.
[18] B. Kenzhaliyev, T. Surkova, A. Berkinbayeva, L. Amanzholova, B. Mishra, B. Abdikerim, D. Yessimova, Modification of natural minerals with technogenic raw materials, *Metals*, 2022, **12**(11), 1907, doi: 10.3390/met12111907.
[19] G. Falini, M. L. Basile, S. Gandolfi, F. Carella, G. Guarini, L. D. Esposti, M. Iafisco, A. Adamiano, Natural calcium phosphates from circular economy as adsorbent phases for the remediation of textile industry waste-waters, *Ceramics International*, 2023, **49**, 243-252, doi: 10.1016/j.ceramint.2022.08.337.
[20] I. S. Cardakli, Green chemistry approaches to extracting calcium phosphate from fish bone wastes, *Ceramics - Silikaty*, 2024, **68**(4), 565-572, doi: 10.13168/cs.2024.0055.
[21] V. M. Shevko, N. M. Mirkayev, D. K. Aitkulov, A. D. Badikova, Producing a siliceous ferroalloy from a mixture of amorphous rocks, *Results in Engineering*, 2024, **23**, 102754, doi: 10.1016/j.rineng.2024.102754.
[22] Y. Mikhlin, A. Karacharov, Y. Tomashevich, A. Shchukarev, Interaction of sphalerite with potassium n-butyl xanthate and copper sulfate solutions studied by XPS of fast-frozen samples and zeta-potential measurement, *Vacuum*, 2016, **125**, 98-105, doi: 10.1016/j.vacuum.2015.12.006.
[23] S. H. Venäläinen, A. Nousiainen, S. Kanerva, The potential of phosphate mine tailings in the remediation of acidic Pb-contaminated soil, *Soil & Environmental Health*, 2024, **2**, 100112, doi: 10.1016/j.seh.2024.100112.
[24] M. Kunarbekova, Y. Yeszhan, S. Zharylkan, M. Alipuly, U. Zhantikeyev, A. Beisebayeva, K. Kudaibergenov, K. Rysbekov, Z. Toktarbay, S. Azat, The state of the art of the mining and metallurgical industry in Kazakhstan and future perspectives: a systematic review, *ES Materials & Manufacturing*, 2024, **25**, doi: 10.30919/esmm1219.
[25] Z. Azhikhanova, M. E. Duru, S. Kucukaydin, H. K. Megbenu, M. Tas Kucukaydin, G. Baisalova, M. Shaimardan, N. Nuraje, M. Ali Özler, Phytochemical profiling and various biological activities of Phlomis tuberosa L, *Scientific Reports*, 2025, **15**, 7293, doi: 10.1038/s41598-024-80456-5.
[26] S. L. Kim, H. Yang, S. Lee, S.-K. Cho, C.-G. Lee, S. Azat, J. Lee, Mining waste as heterogeneous catalysts, *Green Chemistry*, 2025, **27**, 8691-8709, doi: 10.1039/d5gc01509j.
[27] S. University, A. Raimbekova, S. Kubekova, S. University, V. Kapralova, S. University, I. Motovilov, S. University, G. Ibraimova, S. University, N. Ikhsan, S. University, V. Kuznetsov, S. University, Investigation of possibility of manganese ore concentration wastes involvement in inorganic materials production, *Chemical Journal of Kazakhstan*, 2024, 46-56, doi: 10.51580/2024-4.2710-1185.47.
[28] ASTM B748-90(2001)- Standard Test Method for Measurement of Thickness of Metallic Coatings by Measurement of Cross Section with a Scanning Electron Microscope, 2001.
[29] N.-S. Mussa, K. Askaruly, K. Bexeitova, S. Azat, K. Toshtay, Recent advancements in MXene-based catalysts: synthesis, characterization, and applications in sustainable energy production, *Carbon Trends*, 2025, **20**, 100551, doi: 10.1016/j.cartre.2025.100551.

Publisher's Note: Engineered Science Publisher remains neutral with regard to jurisdictional claims in published maps and institutional affiliations.

Open Access
This article is licensed under a Creative Commons Attribution 4.0 International License, which permits the use, sharing, adaptation, distribution and reproduction in any medium or format, as long as appropriate credit to the original author(s) and the source is given by providing a link to the Creative Commons license and changes need to be indicated if there are any. The images or other third-party material in this article are included in the article's Creative Commons license, unless indicated otherwise in a credit line to the material. If material is not included in the article's Creative Commons license and your intended use is not permitted by statutory regulation or exceeds the permitted use, you will need to obtain permission directly from the copyright holder. To view a copy of this license, visit http://creativecommons.org/ licenses/by/4.0/.

©The Author(s) 2025.